MODELLING THE FATIGUE CRACK GROWTH USING THE CRACK TIP PLASTIC DEFORMATION

D.M. Neto[1*], E.R. Sérgio[1], F.V. Antunes[1]
[1] University of Coimbra, CEMMPRE, Department of Mechanical Engineering,
Rua Luís Reis Santos, Pinhal de Marrocos, 3030-788 Coimbra, Portugal
[*] Contact person: diogo.neto@dem.uc.pt

RESUMEN

Este estudio presenta un modelo de elementos finitos para predecir la tasa de crecimiento de grieta por fatiga (FCG) en probetas del tipo Compact-Tension (CT) sometidas a cargas cíclicas tanto de amplitud constante como variable. El material estudiado es la aleación de titanio Ti-6Al-4V. El modelo numérico utiliza la deformación plástica en el vértice de la grieta para definir la liberación nodal y la consiguiente propagación de grieta. Las predicciones numéricas de la tasa de FCG para cargas de amplitud constante concuerdan bien con las mediciones experimentales, lo que indica que la deformación plástica cíclica es el principal mecanismo de daño. En el caso de sobrecargas simples, los resultados numéricos muestran que el cierre de grieta es responsable del efecto de las sobrecargas en el comportamiento de la tasa de FCG. El mismo comportamiento se observa en los bloques de carga baja-alta y alta-baja. El comportamiento transitorio observado entre bloques de carga de diferente amplitud se reduce fuertemente o desaparece cuando se desprecia el contacto entre los flancos de grieta en el modelo. Por lo tanto, el cierre de grieta puede explicar el retardo tanto en sobrecargas simples como en patrones de carga alta-baja.

PALABRAS CLAVE: Crecimiento de grietas por fatiga; Deformación plastica; Cierre de grietas; Carga de amplitud variable

ABSTRACT

This study presents a finite element model to predict the fatigue crack growth (FCG) rate in compact tension specimens under both constant and variable amplitude cyclic loadings. The material studied is the Ti-6Al-4V titanium alloy. The numerical model uses the plastic strain at the crack tip to define the nodal release and consequent crack propagation. The numerical predictions of the FCG rate for constant amplitude loading are in good agreement with the experimental measurements, which indicates that cyclic plastic deformation is the main damage mechanism. In case of single overloads, the numerical results show that crack closure is responsible for the effect of overloads on FCG rate behaviour. The same behaviour is observed in the low-high and high-low load blocks. The transient behaviour observed between loading blocks of different amplitude is strongly reduced or vanishes when the contact of crack flanks is neglected in the model. Thus, the crack closure is able to explain the retardation in both single overloads and in high-low load patterns.

KEYWORDS: Fatigue crack growth; Plastic deformation; Crack closure; Variable amplitude loading

INTRODUCTION

Mechanical components submitted to cyclic loading are prone to failure by fatigue. Thus, design against fatigue is fundamental. Assuming the presence of defects in the components, the damage tolerance approach is suitable to study fatigue life in those components. Fatigue crack growth (FCG) is commonly studied experimentally assuming that the stress intensity factor range ΔK is the crack driving force [1]. However, the obtained da/dN-ΔK curves cannot be used to predict the effect of stress ratio or variable amplitude loading. Alternative approaches have been proposed, such as crack closure phenomenon [2] or CJP model [3], but always keeping ΔK as the main parameter.

Although most of the studies are carried out under constant amplitude loadings, real components are typically submitted to complex loading patterns. Hence, different standard load patterns have been proposed, such as TWIST and FALSTAFF sequences for aircrafts [4]. However, there is a high complexity associated with these standard load patterns. Accordingly, the study of overloads, underloads and load blocks is an important forward step to understand the underlying mechanisms under variable amplitude loading conditions. The finite element simulation of the FCG crack tip phenomena has been adopted with success, where the crack tip plastic deformation is usually assumed to be the main mechanism behind FCG [5].

The main goal of this study is the analysis of FCG in the Ti-6Al-4V alloy using the finite element method. The numerical model for the crack growth is based on the plastic strain at the crack tip. The numerical results are compared with the experimental ones to validate the numerical approach. Besides, models with and without contact of crack flanks were considered to isolate the effect of crack closure phenomenon on the FCG.

FINITE ELEMENT MODEL

In the present study, the fatigue crack growth was analysed using the in-house finite element code DD3IMP, which was originally developed to simulate sheet metal forming processes [6]. The numerical model considers the elasto-plastic behaviour of the specimen, which is loaded under quasi-static conditions.

2.1. Material constitutive model

The elasto-plastic behaviour of this material (Ti-6Al-4V) is modelled by a phenomenological constitutive model. The elastic behaviour is described by the Hooke's law. Regarding the plastic behaviour, the von Mises yield criterion is adopted to define the material yielding. The isotropic work hardening of the titanium alloy is described by the Swift law, given by:

$$Y = K(\varepsilon_0 + \bar{\varepsilon}^{\mathrm{p}})^n \quad \text{with} \quad \varepsilon_0 = \left(\frac{Y_0}{K}\right)^{1/n}, \tag{1}$$

where $\bar{\varepsilon}^{\mathrm{p}}$ denotes the equivalent plastic strain. The parameters of the Swift law are K, ε_0 and n. The kinematic hardening behaviour is described by the Armstrong-Frederick model [7], defined by:

$$\dot{\mathbf{X}} = C_X \left(X_{sat} \frac{\boldsymbol{\sigma}' - \mathbf{X}}{\bar{\sigma}} - \mathbf{X} \right) \dot{\bar{\varepsilon}}^{\mathrm{p}}, \tag{3}$$

where $\boldsymbol{\sigma}'$ is the deviatoric Cauchy stress tensor, $\mathbf{X}$ is the back-stress tensor and $\bar{\sigma}$ is the von Mises stress. C_X and X_{sat} are the kinematic hardening parameters.

Both the isotropic and kinematic hardening parameters were simultaneously calibrated using the stress–strain curve of the experimental low cycle fatigue test [8]. The calibration of the parameter was carried out based on the minimization of the differences between numerically and experimentally measured values of stress. The obtained parameters are listed in Table 1.

Table 1. Material parameters used in Swift isotropic hardening law coupled with the Armstrong–Frederick kinematic hardening law to describe the plastic behaviour of Ti-6Al-4V.

Material	Y_0 [MPa]	K [MPa]	n	C_X	X_{sat} [MPa]
Ti-6Al-4V	823.5	707.1	-0.029	104.3	402.0

2.2. Specimen and boundary conditions

The study of fatigue crack growth is carried out using CT specimens. Only the upper part of the specimen was simulated since it presents geometric, material and loading symmetry. The finite element mesh is composed by linear hexahedral finite elements. However, only the region near the crack tip is refined to reduce the computational cost. The element size in this zone is 8 μm, which will be the increment size of the crack propagation. The contact of the crack flanks is simulated using a rigid surface at the symmetry plane. This surface can be removed in order to assess the importance of the crack closure on the FCG.

The crack length is defined by applying adequate boundary conditions at the symmetry plane. The values of initial crack sizes adopted this study were 7 mm, 10 mm, 13 mm, 16 mm, 19 mm, 22 mm and 24 mm. Thus, using the same load range (47.13 N) it is possible to cover a wide range of stress intensity factor range. Besides, plane stress conditions are adopted in the numerical model, using a single layer of elements in the thickness direction to reduce the computational effort. The specimen thickness was significantly reduced to 0.1 mm to obtain plane stress conditions using solid finite elements.

2.3. Fatigue crack growth

Crack propagation occurs by releasing the boundary condition of the crack tip element, i.e., the crack tip node is debonded at the instant of minimum load, allowing to simulate the advance of the crack tip. The crack increment is defined by the finite element size (8 μm) present in the zone of the crack path. The adopted fatigue crack growth criterion is based on cumulative plastic deformation, which is assumed to be the main crack driving force [9].

The plastic strain is evaluated at the crack tip, which is compared with a critical value of the material under analysis, defining the number of load cycles required to produce a crack propagation. The predicted FCG rate is the ratio between the crack increment (8 μm) and the number of load cycles required to achieve the critical value of cumulative plastic strain at the crack tip. The crack tip node is released when the plastic strain achieves the critical value. The critical value of cumulative plastic strain was calibrated for this titanium alloy [8]. The idea behind the calibration procedure is to reduce the difference between numerical and experimental FCG rate. For this titanium alloy, the obtained value was 153%.

RESULTS AND DISCUSSION

The comparison between experimental and predicted da/dN-ΔK curves is presented in Figure 1 for stress ratio of R=0.05. For each value of initial crack length, the predicted FCG rate presents a transient effect at the beginning of the crack propagation. This is related with the formation of residual plastic wake. Therefore, values of FCG rate shown in Figure 1 were evaluated in the steady state regime. Globally, the numerical results are in very good agreement with the experimental ones.

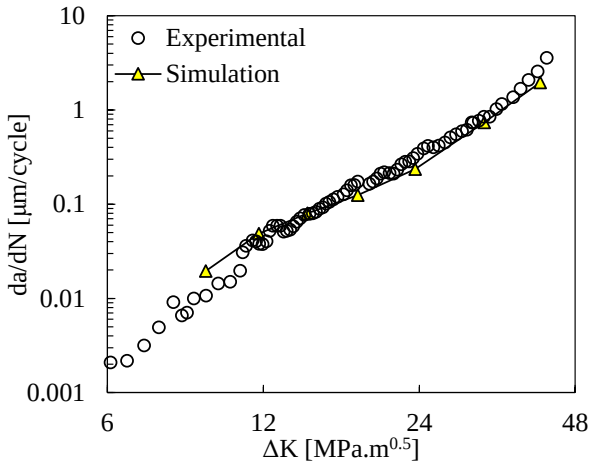

Figure 1. Comparison between experimental and predicted da/dN-ΔK curves for Ti-6Al-4V assuming plane stress conditions in the simulation and R=0.05.

The effect of the overload ratio (OLR) on the predicted FCG rate is presented in Figure 2 (a) for a single overload applied at a_{OL}=16.12 mm of crack length (ΔK_{BL}=18.3 MPa·m$^{0.5}$), considering plane stress conditions. Negative values of ($a-a_{OL}$) denote the crack propagation before the overload application, which is required to stabilize the plastic wake. Except for OLR=2.0, all situations present the same behaviour: a sudden increase of the FCG rate followed by a decrease to a minimum value, which is reached at some point ahead of the overload application and finally a gradual approximation to the constant amplitude crack growth level. This effect predicted numerically is similar to the one observed experimentally in the QSTE340TM steel [10] and 6082-T6 aluminium alloy [11]. On the other hand, crack arrest is observed numerically for OLR=2.0 (Figure 2). Indeed, non-propagating cracks after an overload have been observed experimentally by different authors [12] finding that plasticity-induced crack closure is the main cause of retardation.

The effect of the overload ratio on crack length evolution is presented in Figure 2 (b) for a single overload at a_{OL}=16.12 mm of crack length (ΔK_{BL}=18.3 MPa·m$^{0.5}$), considering plane stress conditions. The increase of the overload ratio leads to an increase of the number of delay cycles. Besides, the relationship between OLR and delay cycles is approximately exponential, ranging between 250 cycles for OLR=1.25 and 5100 cycles for OLR=1.75. In the numerical simulation, the crack stops when there is no increment of plastic deformation at the crack tip, which occurs only for OLR=2.0. This occurs due to the high level of crack closure under this condition.

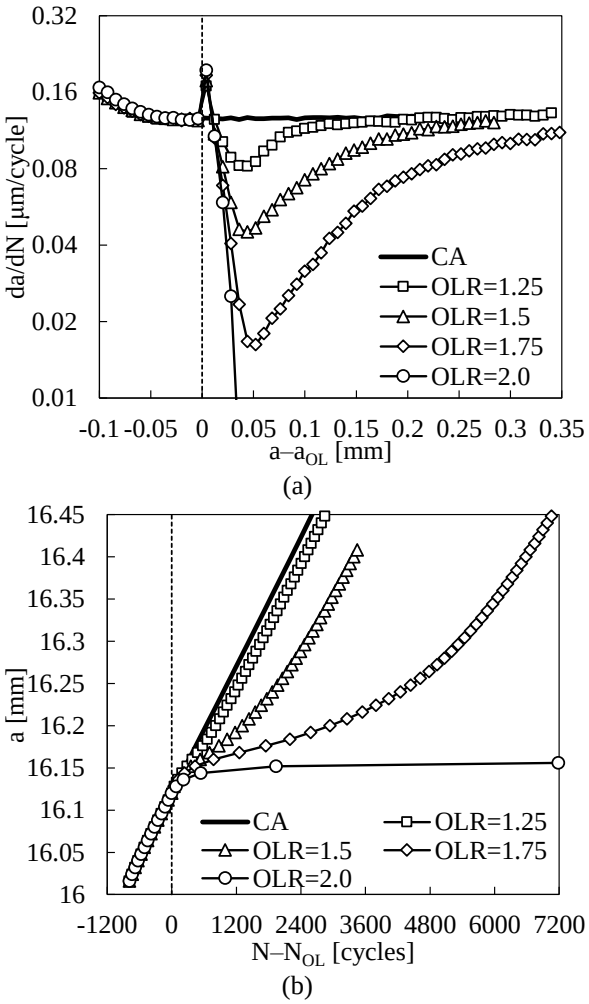

Figure 2. Effect of the overload ratio (OLR) in a single overload (ΔK_{BL}=18.3 MPa·m$^{0.5}$): (a) predicted FCG rate; (b) predicted crack length evolution.

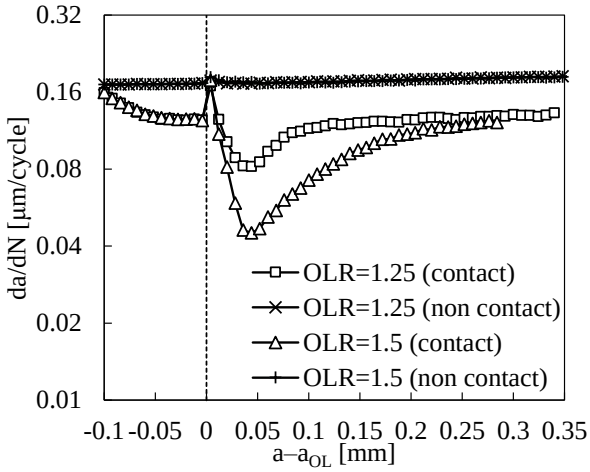

Figure 3. Effect of the contact between crack flank on the predicted FCG rate for a single overload considering a stress ratio R=0.05.

Figure 3 compares the FCG rate for a single overload at a_{OL}=16.12 mm of crack length (ΔK_{BL}=18.3 MPa·m$^{0.5}$), obtained with and without contact of crack flanks. When the contact is removed, the effect of the overload on the FCG rate is negligible. Only a small peak of da/dN is observed when the overload is applied. The FCG rate converges to the constant amplitude crack growth level, i.e. progressive increase of da/dN with crack length. Besides, the evolution of FCG rate in OLR=1.25 and 1.5 are overlapped, indicating insensitive from the overload ratio on the propagation. On the other hand, the inclusion of crack closure produces a dramatic effect on the FCG rate, obtaining typical variation of da/dN associated with an overload. The difference of FCG observed before and after the overload is due to the crack closure, which produces the major effect on the da/dN evolution. Thus, the inclusion of contact of crack flanks in the numerical models is fundamental to obtaining accurate and reliable predictions, particularly under variable amplitude loading conditions.

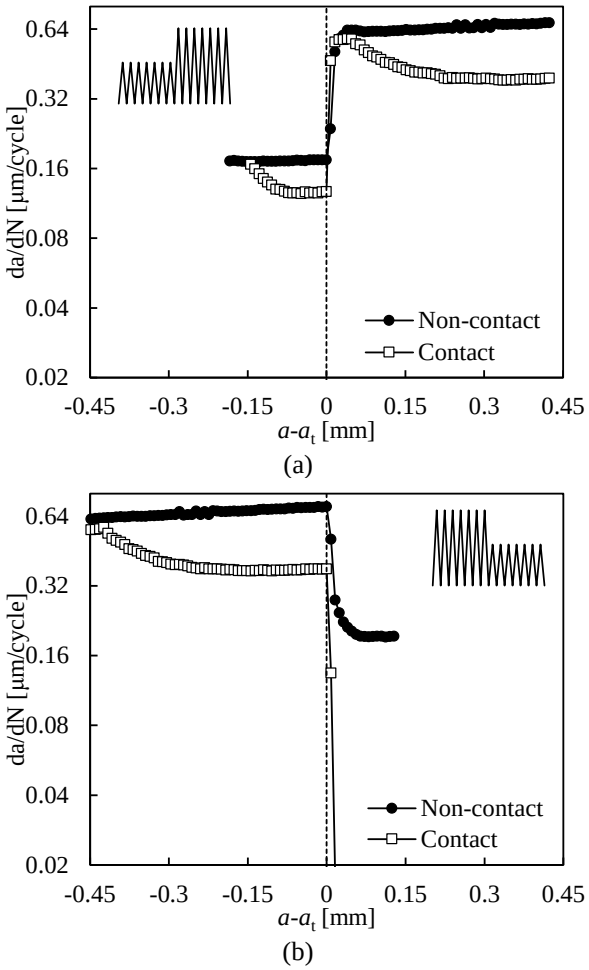

Figure 4. Predicted FCG rate for two different load blocks, comparing the situation with and without contact of crack flanks: (a) low-high load pattern; (b) high-low load pattern.

Figure 4 (a) presents the evolution of the predicted FCG rate for a low-high load block (minimum load identical in both blocks), comparing the situation with and without contact at the crack flanks. The relative crack length ($a-a_t$) is adopted to simplify the comparison, where a_t denotes the crack length at the transition between loading blocks. The FCG rate predicted by the model that neglects the contact of the crack flanks is globally higher. In fact, the initial decrease of da/dN with crack propagation only occurs if the contact of the crack flanks is considered. This is related to crack closure phenomenon, which is motived by the residual plastic wake. The transient behaviour observed after the block transition extents approximately 0.3 mm when the contact of crack flanks is taken into account. On the other hand, without contact of crack flanks there is no transient regime i.e. the da/dN increases progressively with the crack growth during the load of the second block.

The evolution of the predicted FCG rate for a high-low load block (minimum load identical in both blocks) is presented in Figure 4 (b), comparing the situation with and without contact at the crack flanks. The first load block of the high-low load pattern is identical to the second load block of the low-high load pattern. Neglecting the contact between the crack flanks, the predicted da/dN shows a gradual increase during the first load block. On the other hand, a transient behaviour is observed for da/dN at the beginning of the crack propagation when the contact of the crack flanks is considered. The crack propagation stops immediately after the transition between loading blocks. This behaviour was previously observed experimentally for this load pattern [13]. Nevertheless, removing the contact between the crack flanks, da/dN shows a sudden decrease until achieving the steady state regime. Therefore, the crack stops only due to crack closure phenomenon.

CONCLUSIONS

This study presents a finite element model to predict FCG in CT specimens made of Ti-6Al-4V, which assumes that crack tip plastic deformation is the crack driving force. The crack propagation occurs by nodal release when the plastic strain at the crack tip achieves a critical value. This value is calibrated using a single experimental value of da/dN. Both constant and variable amplitude loadings were studied numerically, namely the application of a single tensile overload and different load blocks.

The FCG rate presents a transient behaviour at the beginning of the crack propagation, which is related with the stabilization of residual plastic wake. During this stage the crack closure level increases. Considering the constant amplitude loading, the numerical predictions are in very agreement with the experimental results, indicating that cyclic plastic deformation is the main mechanism responsible for crack propagation. The typical variation of da/dN after an overload is accurately captured by the numerical model. Besides, the effect of the overload ratio on the extent of retardation is highlighted in the numerical predictions. Nevertheless, when the contact of crack flanks was removed in the

numerical models, there is no significant effect of overload on the FCG. Both low-high and high-low load sequences were studied. The numerical predictions for the low-high load pattern show an acceleration of crack growth rate above the steady state level expected for the high block, followed by a gradual reduction to the steady state value. In the case of the high-low load pattern, there is a fast and strong reduction of FCG rate, followed by a progressive increase to the steady state corresponding to the low block. However, the transient behaviour observed between loading blocks of different amplitude is strongly reduced or vanishes when the contact of crack flanks is neglected.

ACKNOWLEDGMENTS

This research work was sponsored by national funds from the Portuguese Foundation for Science and Technology (FCT) under the project with reference PTDC/EME-EME/31657/2017 and by European Regional Development Fund (ERDF) through the Portugal 2020 program and the Centro 2020 Regional Operational Programme (CENTRO-01-0145-FEDER-031657) under the project UIDB/00285/2020.

REFERENCES

[1] ISO 12108:2018 - Metallic materials — Fatigue testing — Fatigue crack growth method, (2018).

[2] T.T. Shih, R.P. Wei, A study of crack closure in fatigue, Eng. Fract. Mech., 6 (1974) 19–32.

[3] C.J. Christopher, M.N. James, E.A. Patterson, K.F. Tee, Towards a new model of crack tip stress fields, Int. J. Fract. 2008 1484, 148 (2008) 361–371.

[4] P. Heuler, H. Klätschke, Generation and use of standardised load spectra and load–time histories, Int. J. Fatigue, 27 (2005) 974–990.

[5] R. Hamam, S. Pommier, F. Bumbieler, Mode I fatigue crack growth under biaxial loading, Int. J. Fatigue, 27 (2005) 1342–1346.

[6] L.F. Menezes, C. Teodosiu, Three-dimensional numerical simulation of the deep-drawing process using solid finite elements, J. Mater. Process. Technol., 97 (2000) 100–106.

[7] C.O. Frederick, P.J. Armstrong, A mathematical representation of the multiaxial Bauschinger effect, Mater. High Temp., 24 (2007) 1–26.

[8] F.F. Ferreira, D.M. Neto, J.S. Jesus, P.A. Prates, F. V. Antunes, Numerical prediction of the fatigue crack growth rate in SLM Ti-6Al-4V based on crack tip plastic strain, Metals (Basel)., 10 (2020) 1–22.

[9] M.F. Borges, D.M. Neto, F. V. Antunes, Numerical simulation of fatigue crack growth based on accumulated plastic strain, Theor. Appl. Fract. Mech., 108 (2020) 102676.

[10] Y. chao Lu, F. peng Yang, T. Chen, Effect of single overload on fatigue crack growth in QSTE340TM steel and retardation model modification, Eng. Fract. Mech., 212 (2019) 81–94.

[11] L.P. Borrego, J.M. Ferreira, J.M. Pinho da Cruz, J.M. Costa, Evaluation of overload effects on fatigue crack growth and closure, Eng. Fract. Mech., 70 (2003) 1379–1397.

[12] C.S. Shin, N.A. Fleck, OVERLOAD RETARDATION IN A STRUCTURAL STEEL, Fatigue Fract. Eng. Mater. Struct., 9 (1987) 379–393.

[13] L.P. Borrego, J.M. Ferreira, J.M. Costa, Partial crack closure under block loading, Int. J. Fatigue, 30 (2008) 1787–1796.